Open Access Journal

Journal of Power Technologies 96 (4) (2016) 229–237

journal homepage:papers.itc.pw.edu.pl

Analysis on the Operating Characteristic of UHVDC New Hierarchical Connection Mode to AC System

Jun Sun[a], Rong Fu[b,*], Yi Tang[c], WanQian Sun[b], Xiaojuan Huang[b]

[a]*State Key Laboratory of Smart Grid Protection and Control, State Grid Electric Power Research Institute, Nanjing 210000, China;*
[b]*College of Automation, Nanjing University of Posts and Telecommunications, Nanjing 210023, China;*
[c]*College of Electrical Engineering, Southeast University, Nanjing 210003, China*

Abstract

The UHVDC system plays an important role in smart grids. In this paper, a new topology structure of UHVDC hierarchical connection mode to different AC systems is analyzed with a view to improving system transmission abilities. Then a new mathematical model is proposed to calculate the MIIF under different UHVDC hierarchical connection modes. The effect of coupling impedance, equivalent impedance and different DC control mode adopted by two group inverters are illustrated to analyze the MIIF. The method to calculate the MISCR of the multi-infeed HVDC system is also applied to HISCR of UHVDC hierarchical connection mode with the MIIF value. In UHVDC hierarchical connection mode, total power to different hierarchical active current layer can be allocated reasonably to change parameter of the received power grid. Thus, the commutation failure can be analyzed according the MIIF change values of UHVDC hierarchical connection mode to the AC system. Therefore, it may increase the risk of commutation failure in the other converter when one converter is in a state of commutation failure. The correctness of the proposed method is verified by PSCAD simulation. The simulation results are illustrated to verify the operating characteristics of the system.

Keywords: UHVDC; Hierarchical Connection Mode; MIIF; HISCR; Commutation failure

1. Introduction

Along with the construction of a strong smart grid and the wide application of ultra high-voltage direct current (UHVDC) transmission technology, the multi-infeed HVDC system plays an important role in the stable operation of the power system. At present, the existing DC access mode may not be conducive to power flow evacuation and would bring a series of voltage support problems for the increasing transmission capacity of DC and the more intensive DC placement. For these reasons, many scholars have conducted in-depth research on the structures, control modes and model building of the HVDC transmission system [1–3]. A new multi-UHVDC hierarchical connection mode to AC systems is put forward to improve the voltage support capability of the received power grid and to result in a reasonable distribution of power flow. The multi-UHVDC hierarchical connection mode involves inverters in a DC line having access to a different voltage level grid, such as 1000 kV and 500 kV. For example, in a Jiangsu multi-UHVDC system, the Xitaimeng-Taizhou UHVDC line will be fed respectively into 1000 kV and 500 kV AC power grids through bipolar DC lines.

Usually, the HVDC control system generally consists of a main control layer, control gate layer and converter control layer. The control modes are: rectifier current, inverter constant extinction angle or constant voltage, rectifier power and inverter constant extinction angle control. In the hierarchical connection method, two sets of converters on the inverter side can take different control modes [4], power can be achieved between the two power grid controlled distributions, improving the power flow distribution of the system.

Compared with the multi-infeed mode [5], the multi-UHVDC hierarchical connection mode has characteristics of low engineering cost and facilitates attempts to increase the voltage support capability of the multi-infeed UHVDC system. In the hierarchical access mode, in order to study the function of coupling between the two loops, the common existing steady-state performances contain the short circuit ratio (SCR) and interaction factor of the multi-infeed interaction factor (MIIF). MIIF means that the interaction between the AC bus voltage can affect the characteristics with rela-

*Corresponding author

Email addresses: sunjun2001@sgepri.sgcc.com.cn (Jun Sun), furong@njupt.edu.cn, 399010550@qq.com (Rong Fu), tangyi@seu.edu.cn (Yi Tang), sunwanqiannj@163.com (WanQian Sun), 15150568465@163.com (Xiaojuan Huang)

tive strengths in the AC system and the commutation failure with the inverter station. According to the literature [6], the MIIF is not only related to the structure parameters of the receiving power grid, but also the DC control methods, and the experimental simulation method is used to evaluate and validate the MIIF. The study [7] proposes an HVDC-interaction-strength index and analyzes the effects of the equivalent impedance of the electrical distance and the AC system on the MIIF.

The literature [8] indicates that short circuit ratio calculation methods of the multi-infeed short circuit radio system (MISCR) can be applied in hierarchical access. The literature [9] provides the theoretical derivation of two MISCR calculation methods which are consistent: one is based on the structure parameters of the power grid to solve, and the other is based on the MIIF solution. Also [10] introduces the relationship between MIIF and MISCR, and shows the interaction effects on the MIIF when using the multi-infeed effective short circuit ratio. As multi-UHVDC hierarchical connection mode is a kind of innovative connection mode, much research and application work needs to be carried out. Therefore, this paper looks at both the analytic formula concerning the MIIF and the influence analysis of different DC control modes on voltage stability of the multi-UHVDC system with hierarchical connection mode.

Commutation failure is a common fault of the UHVDC transmission system. The reasons for commutation failure are mainly linked with the loss of the trigger pulse and AC system fault. A new control strategy proposed in [11] is confirmed to improve the stability of the power grid, as is proved by simulations. When a commutation failure occurs, if the control measures are not reasonable, a continuous commutation failure may result in the failure of the system, which will cause serious consequences. The literature [12, 13] introduces the commutation process of the converter and analyzes the main factors resulting in commutation failure, including relative movement of line voltage across zero caused by the converter bus voltage or asymmetric AC system fault, converter device failure and others. The main cause of commutation failure lies in the converter extinction angle being too small, as the time for reverse voltage of the thyristor is less [14]. For the Multi-infeed System, the paper [15] proposes a critical MIIF. When the MIIF value is greater than the critical value, the phenomenon of a loop happening commutation failure leads to the risk that another loop will also suffer a bigger commutation failure, as validated by the simulation. At present, the measures to reduce commutation failure available are: reducing MIIF, reactive power compensation equipment, suitable main circuit parameters and using the DC control system with an appropriate control method [16]. So through theoretical derivation, this paper also tries to understand how to reduce the risk of commutation failure by adjusting the MIIF value under different DC control methods of the UHVDC system with hierarchical connection mode.

2. The Model for UHVDC Hierarchical Connection Mode to AC

The model for UHVDC hierarchical connection mode to AC is shown in Fig. 1, where the inverters take the form of two groups of 12-pulse converters in series connected to different voltage grade buses with three-winding transformers respectively. The rectifier side of the UHVDC system with hierarchical access is also connected with the three winding transformer in series by two groups of 12-pulse converters in series connected to the same voltage grade bus with three-winding transformers respectively. According to the Fig. 1, compared with the HVDC system, UHVDC with hierarchical connection mode shows the difference on the inverter side which respectively connects to power grids of 1000 kV and 500 kV.

The structure of the control system of the HVDC system is shown in Fig. 2 and Fig. 3.

In Fig. 2, I_{rm} is the measured value of DC current on the rectifier side, I_{rref} is the expected value of DC current on the rectifier side, U_{dm} is the measured value of DC voltage. The DC current value obtained from the VDCOL command is compared with the expected value I_{rref}, and the smaller value is wanted. Then the trigger angle of the rectifier side converter can be obtained through a current regulator.

In Fig. 3, I_{im} is the measured value of DC current on the inverter side, I_{iref} is the expected value of DC current on the inverter side, U_{dref} is the expected value of DC voltage.

The inverter side of the HVDC system adopts the coordination of three control modes, including constant current (not implemented basically) control mode, constant extinction angle control mode (CEC for short) and constant voltage control mode (CVC for short). They obtain a trigger angle signal from the PI controller and then apply the control method which has the minimum trigger angle under the three control modes as the inverter control.

Because of the hierarchical connection mode, the inverter side has two sets of converters that can be controlled flexibly. Moreover, when the rectifier adopts constant current control, the control method of the inverter has two cases. One case is that both 1000 kV and 500 kV buses use CEC or CVC control mode and the other one is either 1000 kV or 500 kV uses CVC control, which means the rest bus adopts the CEC control. Hence there are four adopted kinds of DC control modes in the UHVDC system with hierarchical connection mode.

The following analysis of the hierarchical system includes inverter voltage and power equations. When the system adopts different DC control, the mathematical models and equations are different.

2.1. CEC control mode in inverter

When constant current is adopted on the rectifier side and CEC control modes are adopted in both sets of converters on the inverter side, the equations are as follows:

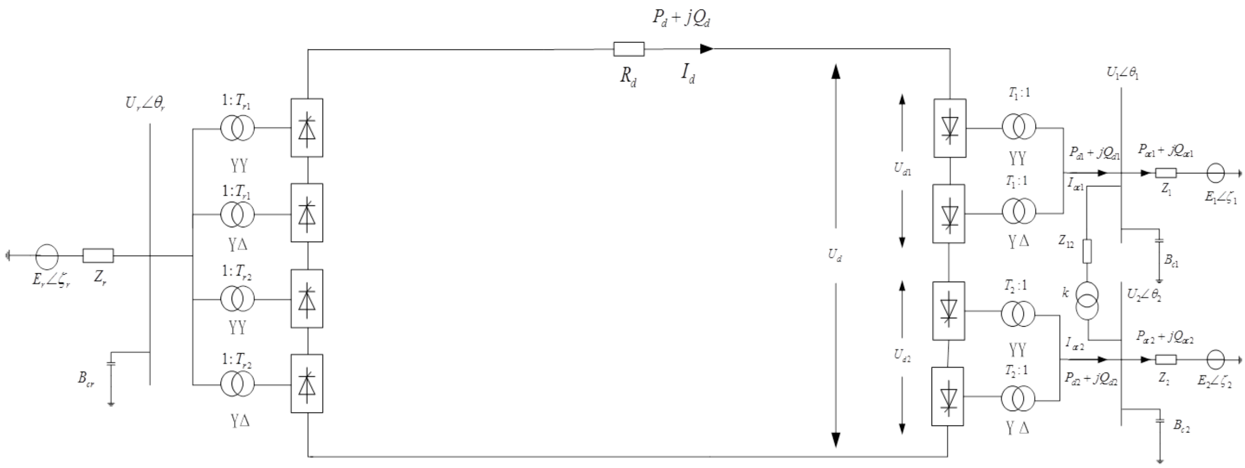

Figure 1: Typical UHVDC hierarchical connection mode to AC system

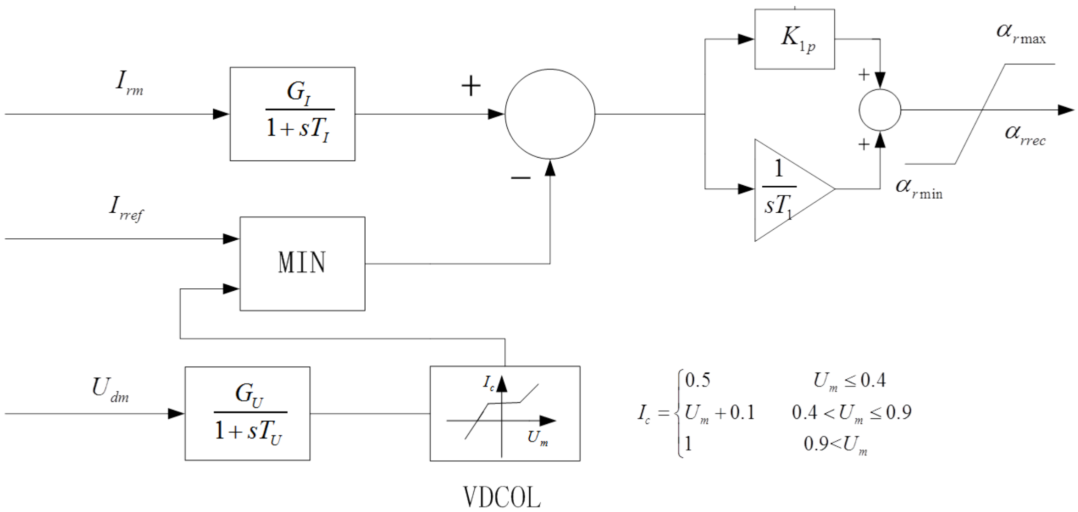

Figure 2: The control system of rectifier side

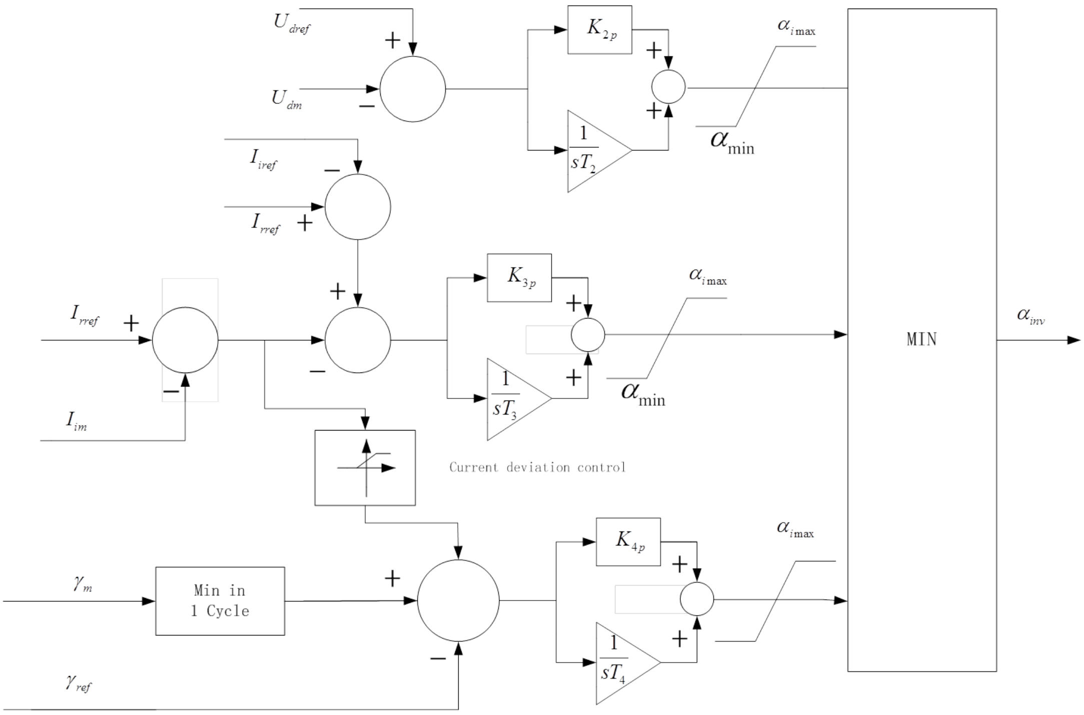

Figure 3: The control system of inverter side

$$\begin{cases} I_d = I_{ref} \\ \gamma_1 = \gamma_2 = \gamma_{ref} \end{cases} \tag{1}$$

where I_d is the DC current of the system, I_{ref} is the expected value of DC current of the system, γ_1 and γ_2 are the value of the extinction angle of two groups of 12-pulse converter, γ_{ref} is the expected value of the extinction angle.

The voltage equation for the inverter side:

$$\begin{cases} U_{doi} = \frac{3\sqrt{2}}{\pi} BT_i U_i \\ U_{di} = U_{doi} \cos\gamma_i - R_{ci} B I_d \\ U_d = U_{d1} + U_{d2} \\ i = 1, 2 \end{cases} \tag{2}$$

where U_{do1} and U_{do2} are ideal no-load voltage of converter devices, U_d is entire inverter side DC voltage, and it is also the sum of U_{d1} and U_{d2}, T_1 and T_2 are the transformer ratio on the inverter side, R_{c1} and R_{c2} are called equivalent commutation resistance, which can be used to explain voltage drop caused by commutation. B is the number of the 6 pulse converter.

The power equation for the inverter side:

$$\begin{cases} P_{di} = U_{di} I_d \\ Q_{di} = -I_d \sqrt{U_{doi}^2 - U_{di}^2} \\ P_d = U_d I_d = P_{d1} + P_{d2} = P_{ac1} + P_{ac2} \\ i = 1, 2 \end{cases} \tag{3}$$

where P_{d1} and P_{d2} are active power received by loop 1 and loop 2 respectively, Q_{d1} and Q_{d2} are reactive power delivering to loop 1 and loop 2 respectively, P_d is active power in the DC transmission line.

2.2. CVC control mode in inverter

When constant current is adopted on the rectifier side and CVC control modes are adopted in both sets of converters on the inverter side, the equations are as follows:

$$\begin{cases} I_d = I_{ref} \\ U_{d1} = U_{d2} = U_{ref} \end{cases} \tag{4}$$

where U_{ref} is the expected value of U_{d1} and U_{d2}.

The voltage equation for the inverter side:

$$\begin{cases} U_{doi} = \frac{3\sqrt{2}}{\pi} BT_i U_i \\ U_{di} = U_{ref} \\ U_d = U_{d1} + U_{d2} \\ i = 1, 2 \end{cases} \tag{5}$$

The power equation for the inverter side:

$$\begin{cases} P_{di} = U_{di} I_d \\ Q_{di} = -I_d \sqrt{U_{doi}^2 - U_{di}^2} \\ P_d = U_d I_d = P_{d1} + P_{d2} = P_{ac1} + P_{ac2} \\ i = 1, 2 \end{cases} \tag{6}$$

3. MIIF for Hierarchical Connection Mode

MIIF is introduced to evaluate the interaction between any two inverter AC voltages. By inducing an approximant 1% step voltage at one converter's AC bus through a switching

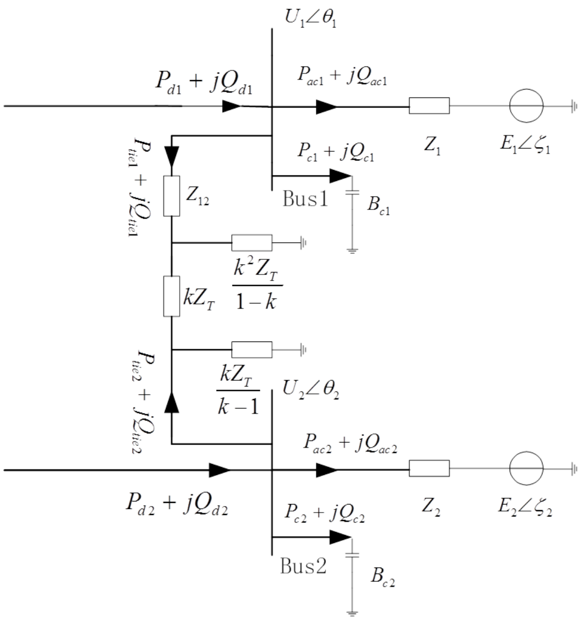

Figure 4: Network nodes of inverter side

connection to three-phase reactors, we observe the voltage reduction at the other converter's AC bus. The ratio of these numbers is the MIIF between the two buses.

$$MIIF_{ij} = \frac{\Delta U_j}{\Delta U_i} \tag{7}$$

where ΔU_j and ΔU_i are the voltage reduction at commutation bus j and bus i. The traditional HVDC transmission usually applies the MIIF to measure the interaction of the multi-infeed HVDC system. In UHVDC hierarchical connection mode, the computation of its MIIF is studied in this paper.

3.1. Power Flow Equation of Converter

When the system is stable, and the three-phase reactors are not put into operation, the power flow equations of the converter in bus 1 and bus 2 are as follows.

$$\begin{cases} P_i = P_i(\theta, U) = U_i \sum_{j=1}^{2} U_j (G_{ij}\cos\theta_{ij} + B_{ij}\sin\theta_{ij}) \\ Q_i = \mathrm{Q}_i(\theta, U) = U_i \sum_{j=1}^{2} U_j (G_{ij}\sin\theta_{ij} - B_{ij}\cos\theta_{ij}) \\ (i = 1, 2) \end{cases} \tag{8}$$

where P_i and Q_i are active power and reactive power injecting into node i, G_{ij} and B_{ij} are conductance and susceptance between node i and j. Due to the different voltage level between the converter buses, the converter buses are connected by transformer of ratio k. The equivalence of the inverter side is shown in Fig4., where Z_T is equivalent impedance to the low voltage side of transformer. Different voltage level buses are connected by transformer of ratio k. Z_1, Z_2 and Z_{12} are equivalent impedance of the AC system and coupled impedance between AC1 and AC2 respectively.

So the admittance matrix of bus 1 and bus 2 is

$$Y = \begin{bmatrix} \frac{1}{Z_1} + \frac{1}{k^2 Z_T + Z_{12}} & -\frac{k}{k^2 Z_T + Z_{12}} \\ -\frac{k}{k^2 Z_T + Z_{12}} & \frac{1}{Z_2} + \frac{-k^2}{k^2 Z_T + Z_{12}} \end{bmatrix} \tag{9}$$

When the three-phase reactor is put on the converter side in bus 2, the power flow equations for bus 1 and bus 2 are changed to:

$$\begin{bmatrix} \Delta P \\ \Delta Q \end{bmatrix} \approx J \begin{bmatrix} \Delta\theta \\ \Delta U \end{bmatrix} \tag{10}$$

3.2. Change of Power Injection in Buses

Not considering the effect of load or injection active power change of each node, the injection change of bus 1 is mainly the reactive power injection change of the DC system and constant voltage source. The equation ((10)) is given as follows:

$$\begin{cases} \Delta P_1 = \Delta P_{d1} + \Delta P_{j1} \\ \Delta P_2 = \Delta P_{d2} + \Delta P_{j2} \\ \Delta Q_1 = \Delta Q_{d1} + Q_{j1} \end{cases} \tag{11}$$

When the mode of the DC control system is different, the power changes ΔP_d and ΔQ_d are different. If we choose Constant current control mode of the rectifier side and CEC control mode of both sets of converters on the inverter side, the power changes are as follows:

$$\begin{cases} \Delta P_{d1} = \frac{3\sqrt{2}}{\pi} B T_1 I_{ref} \cos\gamma_{ref} \Delta U_1 = F \Delta U_1 \\ \Delta P_{d2} = \frac{3\sqrt{2}}{\pi} B T_2 I_{ref} \cos\gamma_{ref} \Delta U_2 = K \Delta U_2 \\ \Delta Q_{d1} = -\Delta P_{d1} \frac{U_{do1} - U_d \cos\gamma_{ref}}{\cos\gamma_{ref} \sqrt{U_{do1}^2 - U_d^2}} = M \Delta U_1 \end{cases} \tag{12}$$

If the Constant current control mode of the rectifier side and CVC control mode of both sets of converters on the inverter side are chosen, the power changes are as follows:

$$\begin{cases} \Delta P_{d1} = 0 \\ \Delta P_{d2} = 0 \\ \Delta Q_{d1} = \frac{3\sqrt{2}}{\pi} T_1 I_d \frac{U_{do1}}{\sqrt{U_{do1}^2 - U_d^2}} \Delta U_1 = M' \Delta U_1 \end{cases} \tag{13}$$

The changes of constant voltage source E_1 and E_2 in active and reactive power injection are as follows:

$$\begin{cases} \Delta P_{ji} \approx (U_i E_i / |Z_i|) \cdot \sin\left(\theta_i + \delta_i - \xi_i\right) \Delta\theta_i - \\ E_i / |Z_i| \cdot \cos\left(\theta_i + \delta_i - \xi_i\right) \Delta U_i \\ \Delta Q_{ji} \approx -(U_i E_i / |Z_i|) \cdot \cos\left(\theta_i + \delta_i - \xi_i\right) \Delta\theta_i - \\ E_i / |Z_i| \cdot \sin(\theta_i + \delta_i - \xi_i) \Delta U_i \\ (i = 1, 2) \end{cases} \tag{14}$$

Then we obtain:

$$\begin{cases} \Delta P_{ji} \approx a_i \Delta\theta_i + b_i \Delta U_i \\ \Delta Q_{ji} \approx c_i \Delta\theta_i + d_i \Delta U_i \\ (i = 1, 2) \end{cases} \tag{15}$$

In this paper, the rectifier side adopts constant current control and both sets of converters on the inverter side use the

CEC control modes. So equation ((11)) can be rewritten as follows:

$$\begin{cases} \Delta P_1 = \Delta P_{d1} + \Delta P_{j1} = (F + b_1)\Delta U_1 + a_1 \Delta\theta_1 \\ \Delta P_2 = \Delta P_{d2} + \Delta P_{j2} = (K + b_2)\Delta U_2 + a_2 \Delta\theta_2 \\ \Delta Q_1 \approx \Delta Q_{d1} + Q_{j1} = (M + d_1)\Delta U_1 + c_1 \Delta\theta_1 \end{cases} \quad (16)$$

3.3. Solution for MIIF

$$\begin{bmatrix} \Delta P_1 \\ \Delta P_2 \\ \Delta Q_1 \\ \Delta Q_2 \end{bmatrix} = \begin{bmatrix} a_1 \\ 0 \\ c_1 \\ 0 \end{bmatrix} \Delta\theta_1 + \begin{bmatrix} 0 \\ a_2 \\ 0 \\ 0 \end{bmatrix} \Delta\theta_2 + \begin{bmatrix} F + b_1 \\ 0 \\ M + d_1 \\ 0 \end{bmatrix} \Delta U_1 + \begin{bmatrix} 0 \\ K + b_2 \\ 0 \\ 0 \end{bmatrix} \Delta U_2 + \begin{bmatrix} 0 \\ 0 \\ 0 \\ 1 \end{bmatrix} \Delta Q_2 = J \quad (17)$$

Then we can obtain:

$$\begin{bmatrix} a_1 - J_{11} & -J_{12} & F + b_1 - N_{11} & 0 \\ -J_{21} & a_2 - J_{22} & -N_{21} & 0 \\ c_1 - H_{11} & -H_{12} & M + d_1 - L_{11} & 0 \\ -H_{21} & -H_{22} & -L_{21} & 1 \end{bmatrix} = G \quad (18)$$

$$\begin{bmatrix} N_{12} \\ N_{22} - (K + b_2) \\ L_{12} \\ L_{22} \end{bmatrix} = X \quad (19)$$

$$\begin{bmatrix} \Delta\theta_1 \\ \Delta\theta_2 \\ \Delta U_1 \\ \Delta Q_2 \end{bmatrix} = G^{-1} X \Delta U_2 = \begin{bmatrix} C_1 \\ C_2 \\ C_3 \\ C_4 \end{bmatrix} \Delta U_2 \quad (20)$$

From equation ((20)) the MIIF can be solved. It can be found that the three-phase reactor has no influence on the MIIF and the MIIF is only related to the parameters of the AC and DC systems.

3.4. Simulation of MIIF

As shown in Fig. 1, the UHVDC hierarchical connection mode to the AC system is simulated in PSCAD platform. The initial values of Z_1, Z_2 and Z_{12} are 20+j47.1 Ω, 20+j47.1 Ω, and 40+j251.2 Ω. Transformer capacity connecting converter bus 1 and bus 2 is 600 MVA, the ratio is 1000/525 and Z_T is 0.18 pu.

In the system, the rectifier side adopts constant current control and both sets of converters on the inverter side use the CEC control modes. Compared with the cases where there is switching of the three phase reactor in bus 2, Fig. 5 and Fig. 6 respectively show the variation of voltage on converter bus 1 and bus 2.

So we can get MIIF_{21}:

$$MIIF_{21} = \frac{\Delta U_1}{\Delta U_2} = 0.2344 \quad (21)$$

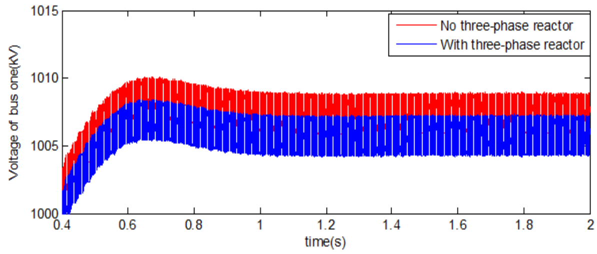

Figure 5: The voltage curve in bus 1

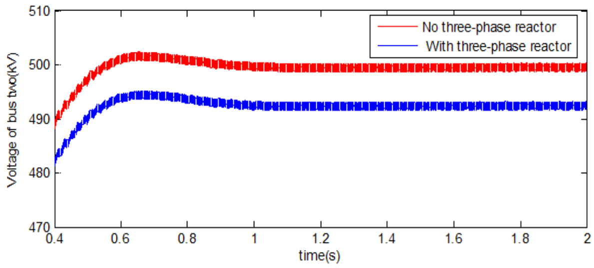

Figure 6: The voltage curve in bus 2

We change the value of Z_1 and Z_2 and do not change the value of Z_{12}. Making comparison between simulations and calculating results from the analytic formula, it is found that the analytic formula for the MIIF is accurate, and the results are given in Table 1.

3.5. Impact factor of MIIF

3.5.1. Impact of electrical distance between bus 1 and bus 2 on MIIF

In hierarchical connection mode, electrical distance between bus 1 and bus 2 is described by coupling impedance Z_{12}. Fig. 7a and 7b show the impact of electrical distance on MIIF_{21} with different DC controls. The initial value of the other parameters and the angle of coupling impedance are kept constant. The initial value of Z_{12} is the base value.

In Fig. 7 it is found that the MIIF decreases with increasing electrical distance. The value of the MIIF is smaller when the rectifier side adopts constant current control and both sets of converters on the inverter side use the CVC control modes.

3.5.2. Impact of equivalent impedance on MIIF

Assuming that the initial value of the other parameters and angle of equivalent impedance are kept constant, Fig. 8 shows the impact of changing the value of equivalent

Table 1: Value of MIIF21 from different equivalent impedance

Simulation conditions	Simulation results	value	Relative error, %
Z_1=15+j47.1 Ω, Z_2=20+j47.1 Ω	0.2253	0.2297	1.95
Z_1=Z_2=20+j47.1 Ω	0.2344	0.2388	1.87
Z_1=20+j47.1 Ω, Z_2=15+j47.1 Ω	0.2324	0.2362	1.63

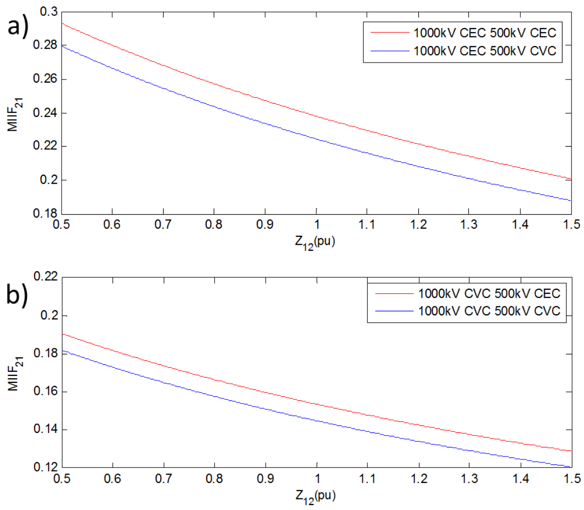

Figure 7: The impact of coupling impedance on MIFF21 with different DC control modes

impedance on the MIIF with different DC control modes. The initial value of Z_1 and Z_2 are the base.

Comparing Z_1 with Z_2, it is found that the change of Z_1 has a great influence on the MIIF. When the rectifier side adopts constant current control and both sets of converters on the inverter side use the CVC control modes, the value of the MIIF is at a minimum.

In addition to electrical distance, the equivalent impedance and the DC control modes, the structure of the DC system, parameters of constant voltage source and the transformer parameters of converter bus also have an impact on the MIIF.

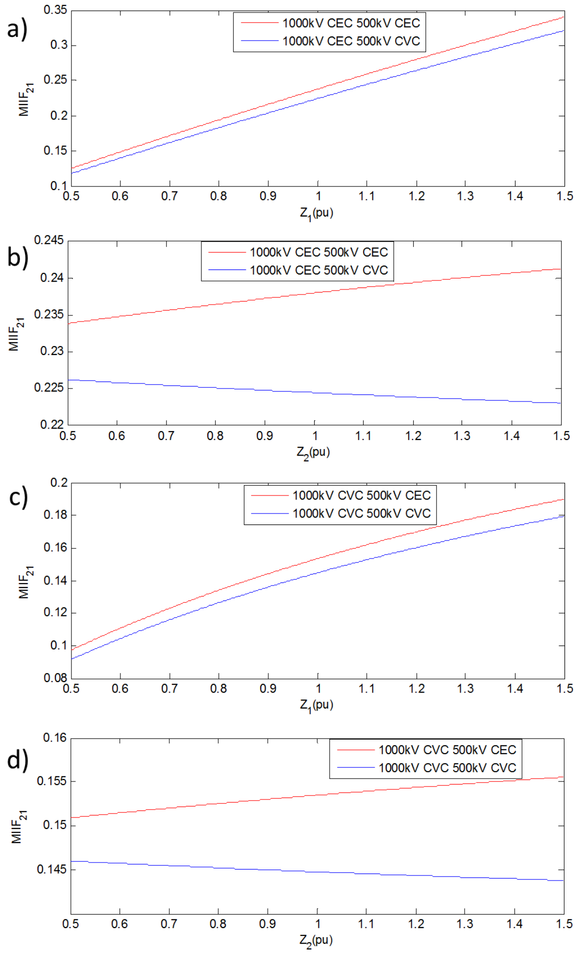

Figure 8: The impact of equivalent impedance on MIFF21 with different DC control modes

4. HISCR of Hierarchical Connection mode

The method for calculating the MISCR of the multi-infeed HVDC system is also applied to the HISCR of UHVDC Hierarchical connection mode. The system is connected to power grids of 1000 kV and 500 kV, so calculation of the HISCR involves calculating the 1000 kV side and the 500 kV side, i.e., the HISCR of two circuits.

$$HISCR_i = \frac{S_{aci}}{P_{di}+\sum_{j=1,j\neq i}^{n} MIIF_{ji} * P_{dj}} = \frac{S_{aci}}{P_{di}+\sum_{j=1,j\neq i}^{n} \frac{\Delta U_j}{\Delta U_i} P_{dj}} = \frac{U_i/|Z_{eqii}|}{P_{di}+\sum_{j=1,j\neq i}^{n} |Z_{eqij}/Z_{eqii}| P_{dj}} \tag{22}$$

The value of i and j are 1 and 2 and the value of i and j are different. S_{aci} is short circuit capacity of i DC circuit. U_i is rated voltage value of converter bus i. P_{di} and P_{dj} are rated active power of i circuit and j circuit in the DC system, Z_{eqii} is self impedance of the node impedance matrix corresponding to bus i of loop i, and Z_{eqij} is the mutual impedance of the node impedance matrix between the loop i and loop j.

So the node impedance matrix can be obtained by inversing the admittance matrix of bus 1 and bus 2.

$$Z = \begin{bmatrix} \frac{Z_i\left[Z_{ij}+k^2(Z_j+Z_T)\right]}{Z_i+Z_{ij}+k^2(Z_j+Z_T)} & \frac{kZ_iZ_j}{Z_i+Z_{ij}+k^2(Z_j+Z_T)} \\ \frac{kZ_iZ_j}{Z_i+Z_{ij}+k^2(Z_j+Z_T)} & \frac{Z_j\left(Z_i+Z_{ij}+k^2Z_T\right)}{Z_i+Z_{ij}+k^2(Z_j+Z_T)} \end{bmatrix} \tag{23}$$

$$\begin{cases} Z_{eqii} = \frac{Z_i\left[Z_{ij}+k^2(Z_j+Z_T)\right]}{Z_i+Z_{ij}+k^2(Z_j+Z_T)} \\ Z_{eqjj} = \frac{Z_j\left(Z_i+Z_{ij}+k^2Z_T\right)}{Z_i+Z_{ij}+k^2(Z_j+Z_T)} \end{cases} \tag{24}$$

From equation ((22)) the value of HISCR is influenced by the MIIF. But the different equivalent impedance, coupling impedance and the different DC control mode can affect the value of MIIF. Not changing the value of equivalent impedance and coupling impedance, the impact of different DC control modes on HISCR are shown below.

The following (Table 2) is the case of HISCR of the 500 kV side. The rectifier uses constant current control and the two sets of converters on the inverter side adopt different DC control methods.

From equation ((22)) we can know that the HISCR is only related to the MIIF if the system parameters are unchanged. The smaller the MIIF is, the larger the HISCR is. When the system chooses Constant current control mode of the rec-

Table 2: Values of HISCR with different DC control methods on 500 kV side

DC control method, kV CVC	$MIIF_{21}$	HISCR
1000, 500	0.2388	2.05
1000, 500	0.2251	2.07
1000, 500	0.1532	2.20
1000, 500	0.1455	2.22

tifier side and CVC control mode of both sets of converters on the inverter side, the MIIF is at a minimum, the HISCR is the largest. It shows that the system is more robust in this control mode.

5. Impact of Power Flow on Commutation Failure

Commutation failure is one of the most common failures in the HVDC system. The fundamental reason for commutation failure is that the extinction angle is too small, so the thyristor has insufficient reverse recovery time and does not have the ability to block. In general, the method for judging commutation failure is to compare inverter extinction angle γ under the condition of AC fault or DC fault with limit extinction angle γ_{min} corresponding to commutation failure. If $\gamma < \gamma_{min}$, commutation failure occurs. Generally, γ_{min} is 7.

In the HVDC system, we can obtain γ from equation ((25)).

$$\gamma = \arccos\left(\frac{\sqrt{2}TX_cI_d}{U} + \cos\beta\right) - \Phi \tag{25}$$

where Φ is zero-crossing phase shift angle, β is advance trigger angle. If the AC system is symmetrical, the value of Φ is zero, and if the AC system is unsymmetrical, the value of Φ is not equal to zero.

When hierarchical connection mode is connected to different voltage levels, extinction angle γ_1 of loop 1 and extinction angle γ_2 of loop 2 are obtained:

$$\begin{cases} \gamma_1 = \arccos\left(\frac{\sqrt{2}BT_1I_dX_C}{U_1} + \cos\beta_1\right) - \Phi_1 \\ \gamma_2 = \arccos\left(\frac{\sqrt{2}BT_2I_dX_C}{U_2} + \cos\beta_2\right) - \Phi_2 \end{cases} \tag{26}$$

If converter bus 1 suffers from reactive power disturbance, extinction angle γ_1 changes. Extinction angle γ_2 also changes because of voltage interaction. New γ_2' is as follows:

$$\gamma_2' = \arccos\left(\frac{\sqrt{2}BT_2I_dX_C}{U_2 - MIIF12 \cdot \Delta U_1} + \cos\beta_2\right) - \Phi_2 \tag{27}$$

From equation ((26)) and ((27)), we know that loop 1 will have commutation failure if the drop of U_1 makes $\gamma_1' < \gamma_{min}$. Because of voltage interaction, U_2 will drop too. If $MIIF_{12}$ is small, loop 2 will not suffer commutation failure because drop of U_2 does not make $\gamma_2' < \gamma_{min}$. Loop 2 will suffer commutation failure if $MIIF_{12}$ is big. When changing the coupling impedance or equivalent impedance, the distribution of AC current I_{ac1} and I_{ac2} on loop 1 and loop 2 will change. It will change the value of P_{ac1} and P_{ac2} and the power flow of the system. So in hierarchical connection mode, we can change

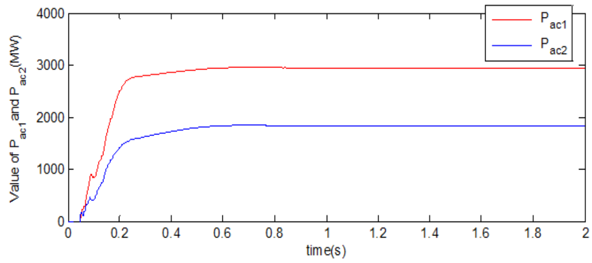

Figure 9: The active power of AC circuit

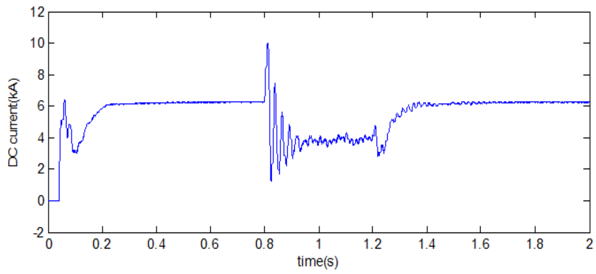

Figure 10: Simulative waveforms for DC current

the extinction angle of loop 1 and loop 2, ratio of converter transformer or parameters of the received system to improve power flow.

If we leave the P_d, U_1, U_2, ratio of the converter transformer and the extinction angle unchanged, the values of active power P_{ac1} and P_{ac2} depend on the parameters of the received system. The initial values of Z_1, Z_2 and Z_{12} are 20+j47.1 Ω, 20+j47.1 Ω, and 40+j251.2 Ω.

From the way to get the MIIF, we know that the parameter of the received system has an impact on the MIIF. So hierarchical connection mode has access to different received systems and it will make active power of every loop different and change the power flow. In Fig. 99, The values of Pac 1 and Pac 2 are approximately 2950 MW and 1900 MW.

The value of $MIIF_{12}$ is 0.1905 when the equivalent impedance and the coupling impedance are unchanged. In this situation the value of MIIF and the voltage drop of U_2 are both low. Under the condition that in 0.8 second converter bus 1 is in a large reactive power disturbance which would be removed in 1.2 second, Gamma indicates the extinction angle, Simulative waveforms for DC current and the

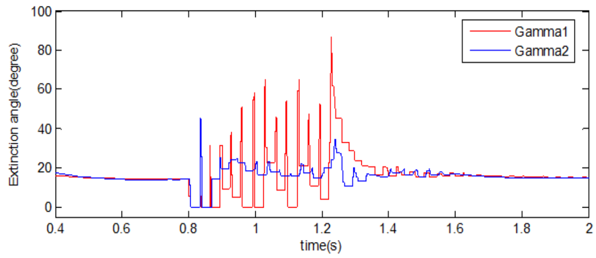

Figure 11: Simulative waveforms for extinction angle

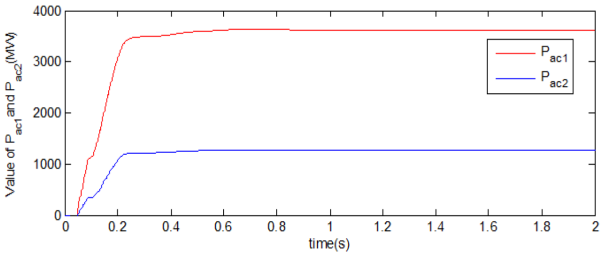

Figure 12: The active power of AC circuit by changing the parameter of the received system

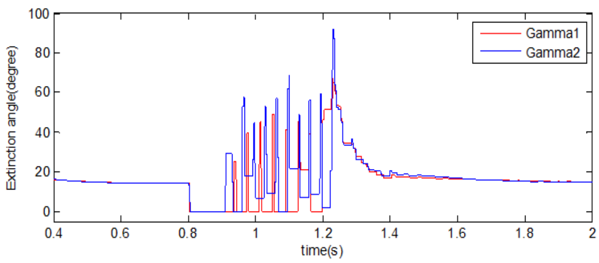

Figure 13: Simulative waveforms for extinction angle by changing the parameter of the received system

extinction angle are shown in Fig. 10 and Fig. 11. Sudden increased DC current caused by the voltage drop of U_1 would lead to commutation failure in loop 2 in a short period of time, and then the inverter in loop 2 could recover from the failure.

If the transformer ratio is changed to 1000/525 and Z_T is 0.1 pu, the value of coupling impedance is 5+j31.4 Ω, the value of MIIF12 is 0.4913, the value of P_{ac1} and P_{ac2} are about 3600 MW and 1250 MW as shown in Fig. 12. The commutation failure in the inverter in loop 1 causes the same situation in the inverter in loop 2. The simulative waveforms extinction angle is shown in Fig. 13.

The simulations show that if the value of MIIF is larger in relative terms, commutation failure in one inverter may lead to communication failure in another inverter.

6. Conclusions

This paper presents a method of solving the multi-infeed interaction factor of UHVDC hierarchical connection mode. The MIIF can accurately depict the voltage interaction of the AC/DC system, and it can be influenced by equivalent impedance of the AC system, coupling impedance between the buses and DC control mode. The HISCR is calculated according to the MIIF. The values of MIIF and HISCR are compared in different control modes on the inverter side.

Hierarchical connection mode has access to different received systems and it can allocate different power flow in the AC system. Simulations were tested to prove that the allocation of power flow and the value of MIIF have an influence on failure in one inverter when commutation failure has already occurred in another inverter.

Acknowledgments

We thank the reviewers for their careful reading of the manuscript and for their very helpful suggestions. Moreover, we are grateful for the financial support we received from Techniques Based on the Trajectory Features and Modes Classification.

References

[1] Y. Han, H. Chen, Y. Lu, L. Li, Research on DC transient overvoltage and insulation coordination of ±800kv converter station, in: Power and Energy Engineering Conference (APPEEC), 2011 Asia-Pacific, IEEE, 2011, pp. 1–4.
[2] F. Wang, H. Li, J. Liu, W. Lu, W. Chen, Q. Long, Analysis of UHVDC transient overvoltage based on the actual control and protection strategy, in: 2014 IEEE PES Asia-Pacific Power and Energy Engineering Conference (APPEEC), IEEE, 2014, pp. 1–4.
[3] M. Saeedifard, R. Iravani, Dynamic performance of a modular multilevel back-to-back HVDC system, IEEE Transactions on Power Delivery 25 (4) (2010) 2903–2912.
[4] G.-h. Ye, Y. Zhang, System static safety analysis under multi-UHVDC hierarchically infeed mode, in: AC and DC Power Transmission, 11th IET International Conference on, IET, 2015, pp. 1–8.
[5] X.-h. Li, F. Long, Z.-x. Cai, L. Zhu, Modeling and analysis of large scale power system with multi-infeed HVDC by EMTDC, in: 2010 Asia-Pacific Power and Energy Engineering Conference, IEEE, 2010, pp. 1–4.
[6] Y. Liu, Z. Chen, Short circuit ratio analysis of multi-infeed HVDC system with a VSC-HVDC link, in: IECON 2011-37th Annual Conference on IEEE Industrial Electronics Society, IEEE, 2011, pp. 949–954.
[7] H. Dai, Y. Wang, X. Li, Z. Ming, H. Deng, Characteristic analysis of reactive power compensation device at HVDC converter station, in: 2012 Asia-Pacific Power and Energy Engineering Conference, IEEE, 2012, pp. 1–5.
[8] L. Weifang, T. Yong, B. Guangquan, S. Yao, Voltage stability analysis of multi-infeed AC/DC power system based on multi-infeed short circuit ratio, in: Power System Technology (POWERCON), 2010 International Conference on, IEEE, 2010, pp. 1–6.
[9] X. Jin, B. Zhou, L. Guan, X. CHENG, Y. ZHANG, HVDC-interaction-strength index for the multi-infeed-HVDC power system, Automation of Electric Power System 33 (2009) 98–102.
[10] X. Chen, A. Gole, M. Han, C. Liu, Influence of the miif index on operation of multi-infeed HVDC systems, in: Electrical Power and Energy Conference (EPEC), 2011 IEEE, IEEE, 2011, pp. 216–221.
[11] Y. Wang, X. Li, C. Wen, Y. He, Impact of AC system strength on commutation failure at HVDC inverter station, in: 2012 Asia-Pacific Power and Energy Engineering Conference, IEEE, 2012, pp. 1–4.
[12] P. Wang, Y. Zhang, H. Chen, X. Li, S. Song, J. Bai, Analysis on the interaction of AC/DC systems based on multi-infeed Q effective short circuit ratio, in: 2012 Asia-Pacific Power and Energy Engineering Conference, IEEE, 2012, pp. 1–4.
[13] Y. Xiaoyu, W. Yuanyuan, G. Weimin, W. Qiang, T. Yaohua, A generator control strategy for reducing the load shedding amount after the UHVDC commutation failure, in: Power System Technology (POWERCON), 2014 International Conference on, IEEE, 2014, pp. 1001–1007.
[14] E. Rahimi, A. Gole, J. Davies, I. Fernando, K. Kent, Commutation failure in single-and multi-infeed HVDC systems, in: AC and DC Power Transmission, 2006. ACDC 2006. The 8th IEE International Conference on, IET, 2006, pp. 182–186.
[15] L. Xin-Nian, L. Yao, L. Tao, C. Shu-Yong, L. Xiao, L. Shao-Bo, Study on the impact of commutation failure on AC voltage of rectifier-side in UHVDC, in: Power System Technology (POWERCON), 2014 International Conference on, IEEE, 2014, pp. 2154–2161.
[16] R. Zhang, C. Zhao, Prony analysis of electrical transient characteristics of AC system during HVDC commutation failure, in: IPEC, 2010 Conference Proceedings, IEEE, 2010, pp. 807–812.